NASA MEMO 12-25-58A

NASA

MEMORANDUM

BOUNDARY-LAYER-TRANSITION MEASUREMENTS ON HEMISPHERES OF VARIOUS SURFACE ROUGHNESSES IN A WIND TUNNEL AT MACH NUMBERS FROM 2.48 TO 3.55

By Angelo Bandettini and Walter E. Isler

Ames Research Center
Moffett Field, Calif.

NATIONAL AERONAUTICS AND SPACE ADMINISTRATION
WASHINGTON
March 1959

1P

NATIONAL AERONAUTICS AND SPACE ADMINISTRATION

MEMORANDUM 12-25-58A

BOUNDARY-LAYER-TRANSITION MEASUREMENTS ON HEMISPHERES OF VARIOUS SURFACE ROUGHNESSES IN A WIND TUNNEL AT MACH NUMBERS FROM 2.48 TO 3.55

A-105

By Angelo Bandettini and Walter E. Isler

SUMMARY

Wind-tunnel tests have been made to determine the location of the boundary-layer transition on three hemispheres having surface roughness (absolute) values of 50, 580, and 2760 microinches. After the initial test run of the smoothest (50 microinch) hemisphere, holes ranging in depth from 1500 to 2500 microinches were noticed in the meridian where transition was observed. The holes were believed to be caused by particles in the air stream. Shadowgraph pictures were obtained of all hemispheres and surface temperature measurements were made on one hemisphere (580 microinches).

Tests at high Reynolds numbers (6.4 to 7.5×10^6) and a Mach number of 2.48 did not indicate any transition on the 50-microinch surface hemisphere before the holes appeared. However, after the holes were noticed, transition locations as low as 50° (measured from the stagnation point) were observed at similar Reynolds numbers and Mach numbers. It is felt the transition resulted from the holes. Similar transition locations of approximately 50° were also observed in the tests of hemispheres with surface roughness values of 580 and 2760 microinches at high Reynolds numbers (6.4×10^6 to 7.5×10^6) and at a Mach number of 2.48. The results at a Mach number of 2.48 indicate that an absolute surface roughness value of 50 microinches was not critical in causing boundary-layer transition at Reynolds numbers of 6.4 to 7.5×10^6 whereas roughness values of 580 and 2760 microinches were greater than critical.

Transition Reynolds numbers based on momentum thickness, R_{θ_T}, varied over a range of approximately 480 to 300 for transition locations, α, on the hemisphere from 88° to 41° (measured from the stagnation point). A maximum value of R_θ of 660 (based on $\alpha = 90°$) was obtained with the 50-microinch surface hemisphere at a Mach number of 2.48.

INTRODUCTION

Bluff shapes having large wave drag have been found to be desirable for reducing the aerodynamic heating of ballistic missiles. In order to calculate the heat transfer to such shapes, a knowledge of the attendant boundary-layer characteristics is necessary. Because of the higher heat-transfer rates characteristic of a turbulent boundary layer, it is desirable to have as long a laminar run as possible. Considerable effort has been expended to produce superfinishes on nose cones in an attempt to insure laminar runs as long as possible. Much research has been done in the past on the effect of roughness on boundary-layer transition for bodies having zero surface pressure gradients such as cones and flat plates. Little, however, is known regarding the effect of roughness in the presence of a favorable pressure gradient, such as is characteristic of bluff shapes.

The investigation reported herein dealt with the location of transition on hemispheres of different roughnesses. A hemisphere was chosen because the surface pressures have been well established both theoretically and experimentally. The stainless-steel hemispheres tested were 19 inches in diameter and 1/8 inch thick. Maximum absolute roughness values of the three hemispheres tested were 50, 580, and 2760 microinches; the corresponding maximum rms values were approximately 15, 150, and 1084 microinches.

The tests were conducted in the 8- by 7-foot supersonic test section of the Ames Unitary Plan wind tunnel at 0° angle of attack at Mach numbers of 2.48, 3.07, and 3.55 and at free stream Reynolds numbers of 1.5×10^{6} to 7.5×10^{6}.

SYMBOLS

D diameter of hemisphere

f' velocity ratio, $\frac{u}{u_e} = \frac{\text{local velocity in boundary layer}}{\text{local velocity outside boundary layer}}$

k surface roughness height

M Mach number

N_{Pr} Prandtl number

p pressure

r	radius
rms	root mean square
R	Reynolds number
R_{∞_D}	free-stream Reynolds number based on diameter, $\frac{\rho_\infty u_\infty D}{\mu_\infty}$
R_e	Reynolds number based on distance along surface and conditions at the outer edge of boundary layer, $\frac{\rho_e u_e S}{\mu_e}$
R_k	Reynolds number based on the absolute roughness height and the velocity, temperature, and viscosity at the absolute roughness height, $\frac{\rho_k u_k k_{abs}}{\mu_k}$
R_θ	Reynolds number based on momentum thickness and conditions at the outer edge of boundary layer, $\frac{\rho_e u_e \theta}{\mu_e}$
s	distance along surface from stagnation point
t	time
T	temperature, $^\circ R$
u	velocity component parallel to surface at point s
α	angular distance from stagnation point, deg
γ	ratio of specific heats, 1.4 for air
δ	boundary-layer thickness
η_{r_l}	$\frac{T_s-T_e}{T_t-T_e}$, local temperature recovery factor (based on surface equilibrium temperature)
θ	momentum thickness
μ	coefficient of viscosity
ρ	air density

Subscripts

abs	absolute or maximum
e	local conditions at outer edge of boundary layer
k	conditions at surface roughness height
rms	root mean square
s	surface
T	transition location
t	total
∞	free-stream conditions

APPARATUS

Wind Tunnel

The tests were conducted in the 8- by 7-foot supersonic test section of the Ames Unitary Plan wind tunnel. It is a closed circuit variable pressure wind tunnel having a flexible wall type nozzle capable of continuous Mach number variations from 2.48 to 3.55. A more detailed description of the wind tunnel is given in reference 1. A survey of the tunnel test section indicates maximum stream angles of 0.25°, which for the purposes of the tests were neglected. Tests on a 10° included angle cone showed a transition Reynolds number (based on free-stream conditions) of about 3.5×10^{6} throughout the Mach number and Reynolds number range.

The models were sting supported from the base. The position of the models in the tunnel was adjustable by means of vertical movement of the support strut so that both the upper and lower surfaces of the models could be viewed and photographed.

Models

Three hemispheres were used in the present investigations. Each of the three models was constructed of stainless-steel and had a diameter of 19 inches and a shell thickness of 1/8 inch. A sketch showing the basic construction features and dimensions is shown in figure 1. Figure 2 is a photograph of the model mounted in the tunnel.

The absolute and rms surface roughness measurements obtained on the hemispheres tested are shown in the following chart.

Model	Surface roughness, microinches	
	abs	rms
A	29-50	10-15
[1]A	29-2500	
D	1000-2760	520-1084
E	[2]580	[2]150

[1]Model A with holes (after first test run in wind tunnel).

[2]Roughness measured from the mean surface line.

Surface roughness measurements were made before the test runs on hemispheres A and D along the meridians where transition was observed and at specific angular locations. Surface measurements were also made after the tests at the same angular and meridian positions and little or no difference between the roughness before and after the tests was observed. However, after the first test run of model "A", holes were noticed near the observed meridian at angular locations of 10°, 25°, and 45°. The maximum depth of the holes was found to be 1750, 1500, and 2500 microinches (abs), respectively. The holes were most likely caused by particles in the air stream and were present when the next set of data hemisphere A was obtained. No roughness measurements were made after the tests with hemisphere E.

A special grit in conjunction with a special lapping process was used to obtain a random three-dimensional surface roughness of uniform height over the complete model surface in the construction of hemispheres A and D. Absolute and rms model surface roughness measurements were made on hemispheres A and D by Ladd Research Industries, Inc., of Roslyn Heights, New York. The method employed to establish the roughness of the model surfaces of hemisphere A consisted of the preparation of surface replicas of collodion. A drop of 4-percent collodion in amyl acetate was put on the surface and allowed to dry. Carbon was then evaporated on the inverted collodion replica forming a replicating film. The collodion was then dissolved in amyl acetate. The carbon film was inverted and large carbon spheres for calibration were placed on the surface replicas. Chromium was vaporized on the specimen at an angle so as to cast shadows of the peaks and holes. The film was examined using an electron microscope. From a comparison of the length of the shadows from the holes and peaks with the length of the shadows from the carbon spheres (diameter known), the depth of the hole and the height of the peaks was determined.

Because of the roughness of the surface on hemisphere D, faxifilm replicas (acetone soluble plastic tape) were made of the surface instead of the usual collodion replicas. Large diameter spheres were placed on flat collodion surfaces alongside the surface replicas and all the surfaces were shadowed with chromium at the same time. Carbon replicas were then made of the faxifilm replicas. All of the replicas made from hemisphere D were then photographed under a standard light microscope.

The surface of hemisphere E was polished to eliminate gross surface irregularities and was then sandblasted to obtain a uniform three-dimensional roughness. Absolute and rms model surface roughness measurements were made with a brush analyzer on a specimen of stainless steel which was subjected to the same sandblasting treatment.

Thermocouples were installed in hemisphere E so that transition on the surface could also be determined by measuring the rise in temperature-recovery factor which is characteristic of boundary-layer transition. In order to obtain temperature readings as close to the surface as possible, stainless-steel inserts 0.011 inch thick and 1/8 inch in diameter were spot-welded in position. Iron-constantan thermocouples were spot-welded to the inserts before being positioned. Surface finishing was done after the 0.011 inserts were welded in place. A typical thermocouple installation is shown in figure 1.

TESTS

Data at a Mach number of 2.48 were obtained over a range of free-stream Reynolds numbers based on hemisphere diameter from 1.5 to 7.5 million, and data at a Mach number of 3.07 were obtained over a range of free-stream Reynolds numbers from 2.8 to 5.8 million. For a Mach number of 3.55, data were obtained only at a free-stream Reynolds number of 3.3 million. All data were obtained with the models at 0° angle of attack.

Transition location was determined on hemispheres A and D from shadowgraphs. Local temperature-recovery values as well as shadowgraph data were obtained on hemisphere E.

METHODS OF DETECTING TRANSITION

Shadowgraph Interpretation

A common method used in detecting transition from a laminar to turbulent boundary layer is the analysis of shadowgraph photographs. The light for the shadowgraphs originated from a spark source with flash durations of 1/4 of a microsecond. The film was approximately 4-1/2 feet from the model.

Transition to turbulent flow is fairly easily identified by the appearance of eddies and the disappearance of the thin diffraction line for bodies like cones and flat plates. However, with models having strong favorable pressure gradients, such as on a hemisphere, it becomes more difficult to detect transition to turbulent flow. This is partially due to the small boundary-layer thickness. Other factors of the investigation reported herein which may tend to hamper good observations are the low-density levels in the test section as well as the large tunnel wall boundary layers.

The indications of transition or turbulent flow used in the present test were:

1. The appearance of a noticeably turbulent wake directly behind the model. Comparison of the wakes of figures 3(a), 3(b), and 3(c) illustrate this condition.

2. The appearance of the boundary layer where it is relatively thick such as along the rearward portion of the body in figure 3(c); an impression of hairiness or a rough surface condition when turbulent eddies cause light to be refracted into the model shadow for a thin boundary-layer condition. This condition may be seen in figure 3(c).

3. The disappearance of the thin diffraction line (fig. 3(a)). The beginning of the turbulent boundary layer in figure 3(c) was determined primarily by the disappearance of the diffraction (outer edge) line. This method of detecting transition has proved quite satisfactory, particularly over two-dimensional flat surfaces such as in the tests of reference 2.

Several independent interpretations of the shadowgraphs for a particular test condition indicated maximum variations in transition location, α_T, of the order of 8°.

To check the methods of observing transition, a strip of No. 60 carborundum having a surface roughness of 0.01 to 0.02 inch was applied at approximately 45° from the stagnation point on the surface of hemisphere A (fig. 1). The boundary layer that was known to be turbulent immediately after the roughness could then be observed and compared with shadowgraph results obtained from laminar flow over a surface.

Local Temperature Recovery Factor

One method which has been found to be very effective in detecting boundary-layer transition on cones and flat plates in supersonic flow is the determination of the temperature recovery factor. Transition is indicated by a very noticeable rise in the value of the temperature recovery factor along the surface in the direction of the air flow. In an

effort to obtain corroboration of the implications of the shadowgraph studies, local temperature-recovery factors were evaluated for hemisphere E using the measured surface temperatures. The temperatures used were those recorded at the same time as the shadowgraph pictures were taken so that a comparison might be made.

The local temperature-recovery factor is by definition

$$\eta_{r_l} = \frac{T_s - T_e}{T_t - T_e} = \frac{\frac{T_s}{T_t}\left[1 + \left(\frac{\gamma-1}{2}\right)M_e^2\right] - 1}{\left(\frac{\gamma-1}{2}\right)M_e^2} \tag{1}$$

In this equation, T_s, is the surface recovery temperature based on adiabatic wall conditions. In this test adiabatic wall conditions were not realized. However, the values of T_s used in computing η_{r_l} are the equilibrium values, that is, $\partial T_s/\partial t = 0$. As the model in question has a relatively thin skin, it is assumed that the measured values of T_s approached the true adiabatic wall temperatures. The local Mach number, M_e, was obtained from an experimental study of Mach number variation over the surface of a hemisphere (ref. 3).

RESULTS AND DISCUSSION

Table I contains a summary of the transition locations as deduced from the shadowgraph pictures for all of the test conditions. Also given in table I are calculated values, at the transition location, of the boundary-layer thickness, δ, the momentum thickness, θ, the Reynolds number based on momentum thickness, R_{θ_T}, the Reynolds number based on length of laminar run, R_{e_T}, and the Reynolds number based on roughness height, R_{k_T}. In instances where no transition was observed on a hemisphere, it could not be determined if transition was imminent at the downstream edge or if laminar flow would have persisted for some distance had there been an afterbody attached to the model. In these cases the value of α_T presented is 90°.

Recovery-Temperature and Shadowgraph Measurements

The temperature data are presented in figures 4 and 5 as the ratio of the wall temperature to the free-stream total temperature. When the temperature data are plotted as temperature recovery factor, as has been done in figures 6 and 7, one characteristic is immediately apparent. This is the divergence from the theoretical values for laminar and

turbulent flow $\left(\text{i.e., } \sqrt{N_{Pr}} \text{ and } \sqrt[3]{N_{Pr}}\right)$ in the region over the forepart of the hemisphere ($0^\circ < \alpha < 45^\circ$). Lower values have also been observed by others (ref. 3) as shown in figure 6(a). In contrast, agreement with the theoretical laminar and turbulent values for recovery factor was obtained on the hemisphere at angles greater than 45° (figs. 6 and 7). When a temperature recovery factor of 0.88 was used to indicate transition to a turbulent boundary layer, good agreement between the two methods of detecting transition was obtained, figure 6(a).

The data obtained for the upper surface of the hemisphere, figures 6(b) and 7(b), indicated approximately the same range of laminar and turbulent recovery-factor values as for the lower surface, figures 6(a) and 7(a). The different location of transition for upper and lower surfaces (fig. 6) may be due to variation in roughness or surface contour between upper and lower surfaces. A large recovery factor (0.935) was also noted on the upper surface at a Reynolds number of 7.5×10^6.

Effect of the Variation of Surface Roughness on Boundary-Layer Transition

Transition locations are shown in figure 8 for different surface roughness values at similar Reynolds numbers and the same Mach numbers. The roughness measurements for hemisphere A are divided into two groups, the measurements made before the holes were discovered (50 microinches), and those made after the holes were discovered (2500 microinches). Results at high Reynolds numbers (6.4 to 7.5×10^6) at a Mach number of 2.48 indicated that an absolute surface roughness of 50 microinches did not cause transition on the smooth hemisphere; however, after the holes were noticed, transition locations as low as 50° (measured from the stagnation point) were observed. It is felt transition resulted from the boundary layer being tripped by the holes. Tests of hemispheres with roughness values of 580 and 2760 microinches also indicated similar transition locations of approximately 50° at high Reynolds numbers (6.4×10^6 to 7.5×10^6) and a Mach number of 2.48. The results at a Mach number of 2.48 indicate that surface roughness values of 580 and 2760 microinches were above critical in causing boundary-layer transition whereas an absolute surface roughness value of 50 microinches was not. Limited data at a Mach number of 3.07 indicate an absolute surface roughness value of 2760 resulted in transition locations of 41° and 55° as compared to 90° with a surface roughness of 580 at Reynolds numbers of 5.3×10^6 and 5.8×10^6.

For approximately the same Reynolds numbers, the transition locations for a constant roughness differed by as much as 35°. The estimated accuracy in detecting transition location for the present investigation is approximately 8° which could account for some of the difference in transition location.

Transition Reynolds Number

In order to correlate the test results with other data, the transition Reynolds numbers were computed on the basis of conditions at the outer edge of the boundary layer and wetted length from the stagnation point, R_{e_T}; and on momentum thickness R_{θ_T}. Reynolds numbers based on the velocity, temperature, and viscosity at the absolute roughness height, and the absolute roughness height, R_{k_T}, were also computed.

The Reynolds numbers of transition based on conditions at the outer edge of the boundary layer were computed using the equation

$$R_e = \left(R_{\infty_D}\right)\left(\frac{s}{D}\right)\left(\frac{p_e}{p_\infty}\right)\left(\frac{M_e}{M_\infty}\right)\left(\frac{T_\infty}{T_e}\right)^{1.26}$$

for which a viscosity-temperature relationship of $\mu \sim T^{0.76}$ was assumed. The variation of R_{e_T} with stream Reynolds numbers for all test models is shown in figure 9. The highest local Reynolds number was 3.2×10^6 ($\alpha_T = 65^\circ$) for a Mach number of 2.48 and 1.9×10^6 ($\alpha_T = 54^\circ$) for a Mach number of 3.07.

The transition Reynolds number based on boundary-layer momentum thickness was computed using the equation

$$R_\theta = \left(R_{\infty_D}\right)\left(\frac{\theta}{D}\right)\left(\frac{p_e}{p_\infty}\right)\left(\frac{M_e}{M_\infty}\right)\left(\frac{T_\infty}{T_e}\right)^{1.26}$$

The momentum thickness used in the above equation was obtained by the method described in references 4, 5, and 6. A maximum value for Reynolds number based on momentum thickness, R_θ, of 660 (for $\alpha = 90^\circ$) was obtained with the 50-microinch surface hemisphere at a free-stream Reynolds number of 7.5×10^6. A curve based on a free-stream Reynolds number of 7.5×10^6 is presented in figure 10 to indicate the variation of R_θ along the surface for this test condition. For the hemispheres with supercritical surface roughnesses (580, 2760, and 50 microinch with holes), the transition Reynolds number, R_{θ_T}, varied from values of approximately 480 to 300 for transition locations on the hemisphere from 88° to 41°, respectively, (fig. 10).

The transition Reynolds numbers, R_{k_T}, based on the velocity, temperature, and viscosity at the absolute roughness height, and on the absolute roughness height, were computed by means of the equation

$$R_k = (R_{\infty_D}) \left(\frac{p_e}{p_\infty}\right) \left(\frac{T_\infty}{T_k}\right)^{1.76} \left(\frac{M_e}{M_\infty}\right) \left(\frac{T_e}{T_\infty}\right)^{0.5} \left(\frac{k_{abs}}{D}\right) (f'_{k_{abs}})$$

The methods used limited the calculations of boundary-layer-thickness values to a maximum location of 69°. The values of f', which is the ratio of (u/u_e), were computed by the methods discussed in references 4, 5, and 6. The maximum transition Reynolds number calculated (321, table I) for the present test was considerably lower than the minimum critical Reynolds number for distributed granular-type roughness (ref. 7) obtained on a cone at supersonic speeds. The lower values of R_{k_T} obtained may be due to the extreme pressure gradients on a hemisphere combined with a surface which was uniformly rough, whereas the data of reference 7 were obtained on smooth surfaces with strips of roughness at various locations. Possibly depressions (holes) rather than protrusions may significantly affect the R_{k_T} values. Also the significant differences in performance between upper and lower meridians may have had some effect. Values of boundary layer and momentum thickness computed by the method of reference 8 were in reasonable agreement with those listed in table I.

CONCLUSIONS

Tests of three hemispheres have been made to determine the effect of maximum surface roughnesses of 50, 580, and 2760 microinches absolute on the location of transition of the boundary layer. After the initial test run of the smoothest (50 microinch) hemisphere, surface holes ranging in depth from 1500 to 2500 microinches were noticed in the region where transition was being observed. The holes are believed to be caused by particles in the air stream. Data at Mach numbers of 2.48, 3.07, and 3.55 and stream Reynolds numbers R_{∞_D} of 1.5 to 7.5×10^6 indicate the following conclusions.

1. At a Mach number of 2.48 and at high Reynolds numbers (6.4 to 7.5×10^6) an absolute surface roughness of 50 microinches did not cause transition on the smooth hemisphere, however, after the holes appeared, transition locations as low as 50° (measured from the stagnation point) were observed. The holes are believed to have caused transition. Tests of hemispheres with roughness values of 580 and 2760 microinches also indicated similar transition locations of approximately 50° at high Reynolds numbers (6.4 to 7.5×10^6) and a Mach number of 2.48. The results indicate that surface roughness values of 580 to 2760 microinches were above critical in causing boundary-layer transition, whereas an absolute surface roughness of 50 microinches was not at a Mach number of 2.48.

2. Transition Reynolds numbers based on momentum thickness, R_{θ_T}, varied from approximately 480 to 300 for transition locations on the hemisphere, α, from 88° to 41° (measured from the stagnation point). The maximum value of R_θ obtained was 660 (based on $\alpha = 90°$) with the 50-microinch surface hemisphere at a Reynolds number of 7.5×10^6 and a Mach number of 2.48.

3. Good agreement between the recovery-temperature and shadowgraph methods of detecting transition was obtained when a temperature recovery factor of 0.88 was used to indicate a turbulent boundary layer.

Ames Research Center
National Aeronautics and Space Administration
Moffett Field, Calif., Aug. 25, 1958

REFERENCES

1. Huntsberger, Ralph F., Jr., and Parsons, John F.: The Design of Large High-Speed Wind Tunnels. NACA Paper presented at Fourth General Assembly of the AGARD Wind Tunnel Panel at Scheveningen, The Netherlands, AG15/P6, May 3-7, 1954.

2. Chapman, Dean R., Kuehn, Donald M., and Larson, Howard K.: Investigation of Separated Flows in Supersonic and Subsonic Streams With Emphasis on the Effect of Transition. NACA Rep. 1356, 1958. (Supersedes NACA TN 3869)

3. Stine, Howard A., and Wanlass, Kent: Theoretical and Experimental Investigation of Aerodynamic-Heating and Isothermal Heat-Transfer Parameters on a Hemispherical Nose With Laminar Boundary Layer at Supersonic Mach Numbers. NACA TN 3344, 1954.

4. Cohen, Clarence B., and Reshotko, Eli: Similar Solutions for the Compressible Laminar Boundary Layer With Heat Transfer and Pressure Gradient. NACA Rep. 1293, 1956. (Supersedes NACA TN 3325)

5. Cohen, Clarance B., and Reshotko, Eli: The Compressible Laminar Boundary Layer With Heat Transfer and Arbitrary Pressure Gradient. NACA Rep. 1294, 1956. (Supersedes NACA TN 3326)

6. Hartree, D. R.: On An Equation Occurring in Faulkner and Skan's Approximate Treatment of the Equations of the Boundary Layer. Proc. Cambridge Phil. Soc., vol. 33, pt. 2, Apr. 1937, pp. 223-239.

7. Braslow, L. Albert: Effect of Distributed Granular-Type Roughness on Boundary-Layer Transition at Supersonic Speeds With and Without Surface Cooling. NACA RM L58A17, 1958.

8. Flügge-Lotz, Irmgard, and Johnson, Arlo F.: Laminar Compressible Boundary Along a Curved Insulated Surface. Jour. Aero. Sci., vol. 22, no. 7, July 1955, pp. 445-454.

TABLE I.- TABULATED DATA FROM TESTS OF THREE HEMISPHERES WITH VARYING SURFACE ROUGHNESS

Model	k_{abs}, micro-inches	M_∞	R_{∞_D} $\times 10^{-6}$	R_∞/ft $\times 10^{-6}$	$\frac{s_T}{r}$	α_T, deg	M_{e_T}	θ_T, $\times 10^3$ in.	R_{θ_T}	R_{e_T} $\times 10^{-6}$	δ_T, $\times 10^2$ in.	R_{k_T}
A	50	2.48	7.57	4.78	1.57	[1]90	2.19	3.10	660.2	2.50		
			7.53	4.75				3.10	658.8	2.49		
			6.47	4.08				3.35	610.3	2.13		
			5.74	3.62				3.56	574.8	1.89		
			5.09	3.21				3.78	541.7	1.68		
			4.43	2.80				4.05	505.2	1.46		
			2.92	1.71				4.98	410.4	.97		
A (holes)	2500	2.48	7.46	4.71	1.13	65	1.57	1.74	509.4	3.18	1.90	
			7.46	4.71	.87	50	1.12	1.32	436.0	2.61	1.38	
			6.40	4.04	1.31	75	1.85	2.23	485.0	2.70		
			6.39	4.03	.93	53	1.19	1.49	419.5	2.39	1.56	
			4.45	2.81	1.57	[1]90	2.19	4.04	506.1	1.47		
			3.04	1.92	1.57	[1]90	2.19	4.85	415.1	.96		
		3.07	5.70	3.60	.94	54	1.27	2.68	375.0	1.91	1.72	
			4.72	2.97	1.54	88	2.30	4.12	482.4	1.55		
			3.31	2.09	1.57	[1]90	2.34	5.78	432.0	1.05		
			2.83	1.78	1.57	[1]90	2.34	6.24	399.3	.89		
E	580	2.48	7.55	4.73	.87	50	1.11	2.31	439.2	2.65	1.36	15.67
			7.02	4.40	.91	52	1.17	2.39	434.6	2.50	1.46	13.03
			6.03	3.78	1.13	65	1.56	2.93	456.6	2.57	2.11	7.35
			4.01	2.51	1.57	[1]90	2.19	4.20	480.0	1.33		
			3.02	1.89	1.57	[1]90	2.19	4.91	417.1	1.00		
		3.07	5.78	3.62	1.57	[1]90	2.34	4.37	570.0	1.83		
			3.99	2.50	1.57	[1]90	2.34	5.26	473.5	1.26		
D	2760	2.48	6.45	4.07	.91	52	1.17	2.45	416.5	2.36	1.52	281.95
			6.45	4.07	.96	55	1.25	2.51	432.3	2.50	1.60	254.73
			6.41	4.04	.84	48	1.07	2.38	392.4	2.15	1.44	320.47
			5.88	3.71	.79	45	.99	2.39	357.0	1.82	1.42	321.10
			5.86	3.70	.87	50	1.12	2.49	387.4	2.05	1.54	261.62
			5.84	3.69	.87	50	1.12	2.49	386.7	2.04	1.55	260.20
			4.52	2.85	1.57	[1]90	2.19	3.98	510.0	1.49		
			4.50	2.84	1.57	[1]90	2.19	3.98	509.2	1.49		
			4.46	2.82	.96	55	1.25	2.85	359.2	1.73	1.96	172.92
			4.45	2.81	1.40	80	1.98	2.96	430.6	1.83		
			1.53	.96	1.57	[1]90	2.19	6.85	296.3	.50		
			1.53	.97	1.57	[1]90	2.19	6.84	297.0	.51		
		3.07	5.25	3.31	.72	41	.93	2.57	300.0	1.33	1.53	235.78
			5.25	3.31	.96	55	1.30	2.81	366.0	1.78	1.85	157.70
			4.79	3.02	1.48	85	2.24	3.59	451.0	1.63		
			4.76	3.00	1.57	[1]90	2.34	4.81	519.1	1.50		
			4.33	2.74	1.57	[1]90	2.34	5.04	495.5	1.37		
			3.76	2.37	1.57	[1]90	2.34	5.42	460.5	1.19		
		3.55	3.32	2.10	1.57	[1]90	2.37	5.47	364.2	1.00		

[1]Laminar flow was observed over the entire hemisphere.

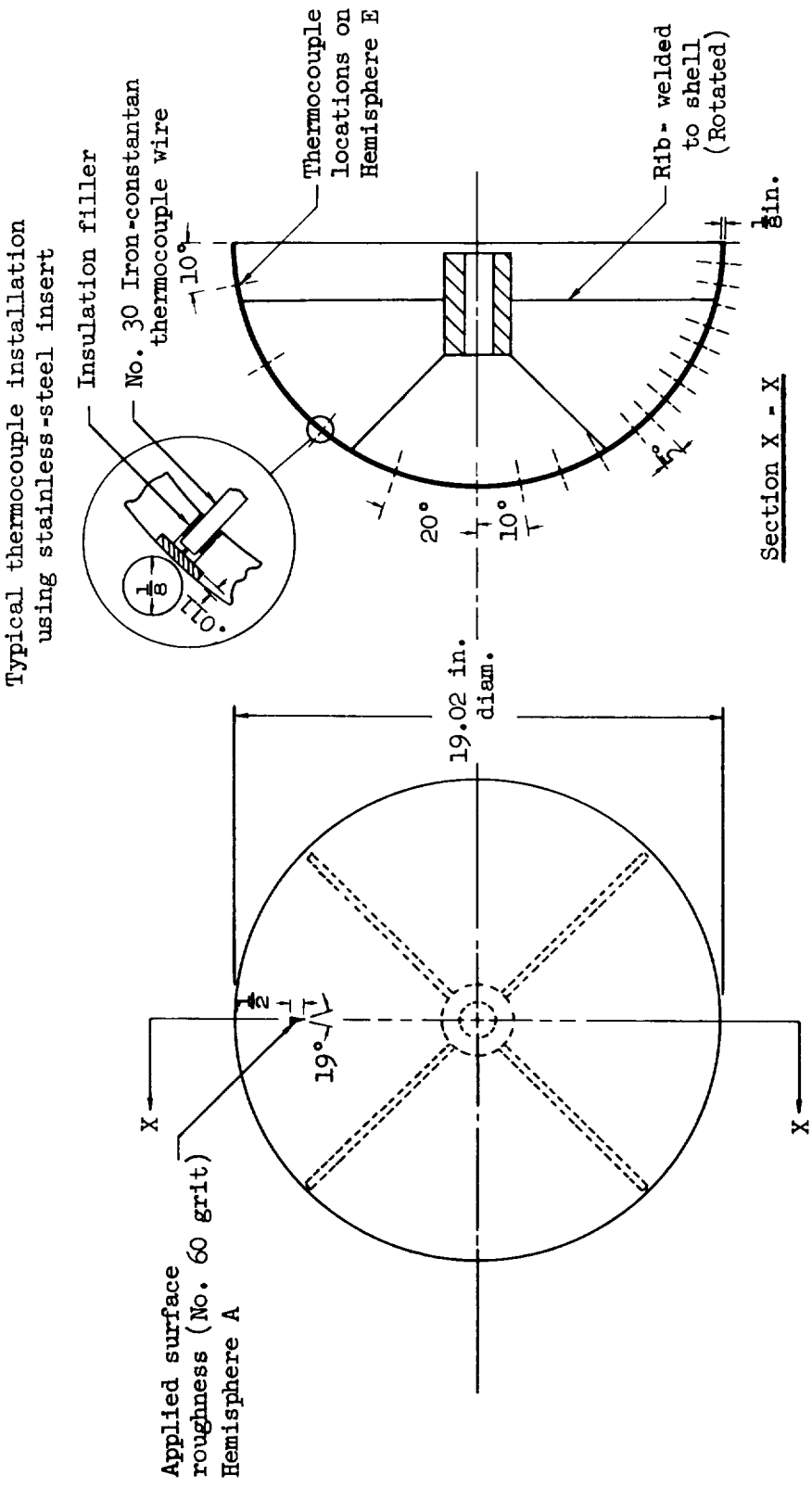

Figure 1.- Sketch showing dimensions of stainless-steel hemispheres and location of thermocouples and applied surface roughness. (All dimensions in inches)

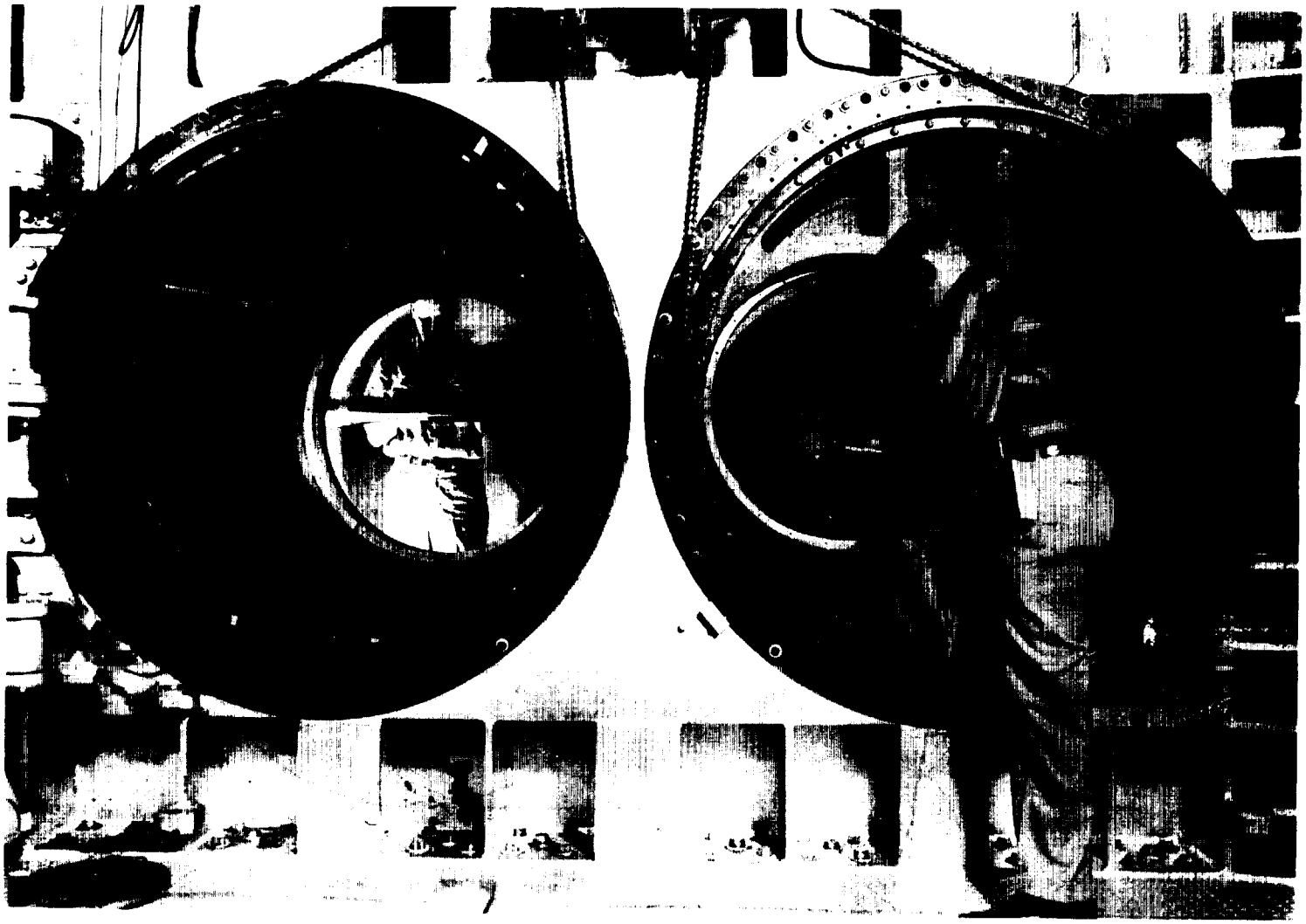

A-21661

Figure 2.- Photograph of a hemisphere in the 8- by 7-foot supersonic test section of the Ames Unitary Plan wind tunnel.

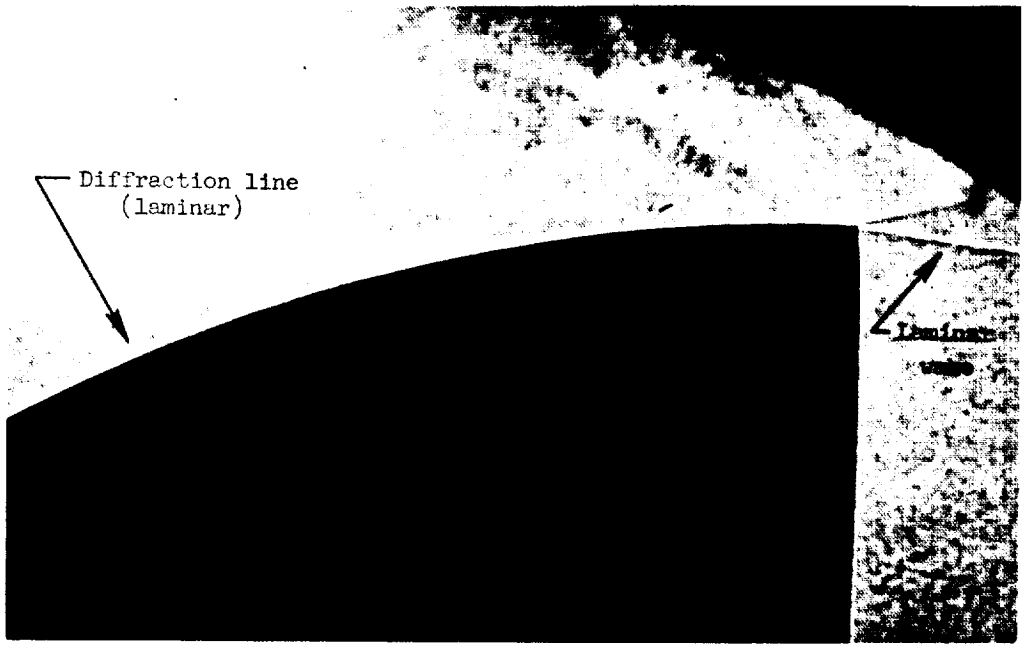

(a) Laminar boundary layer; hemisphere A (after holes); k_{abs} = 2500; M_∞ = 2.48; R_{∞_D} = 4.4×10^6

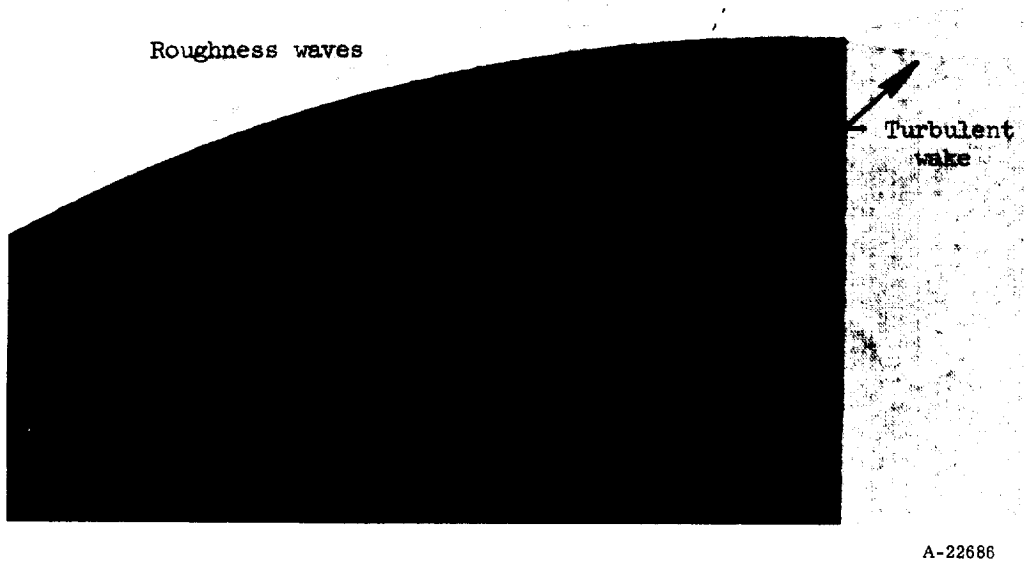

(b) Turbulent boundary layer; hemisphere D, k_{abs} = 2760; M_∞ = 2.48; R_∞ = 6.5×10^6

Figure 3.- Shadowgraphs with indications of laminar and turbulent boundary layers on the surface of a hemisphere.

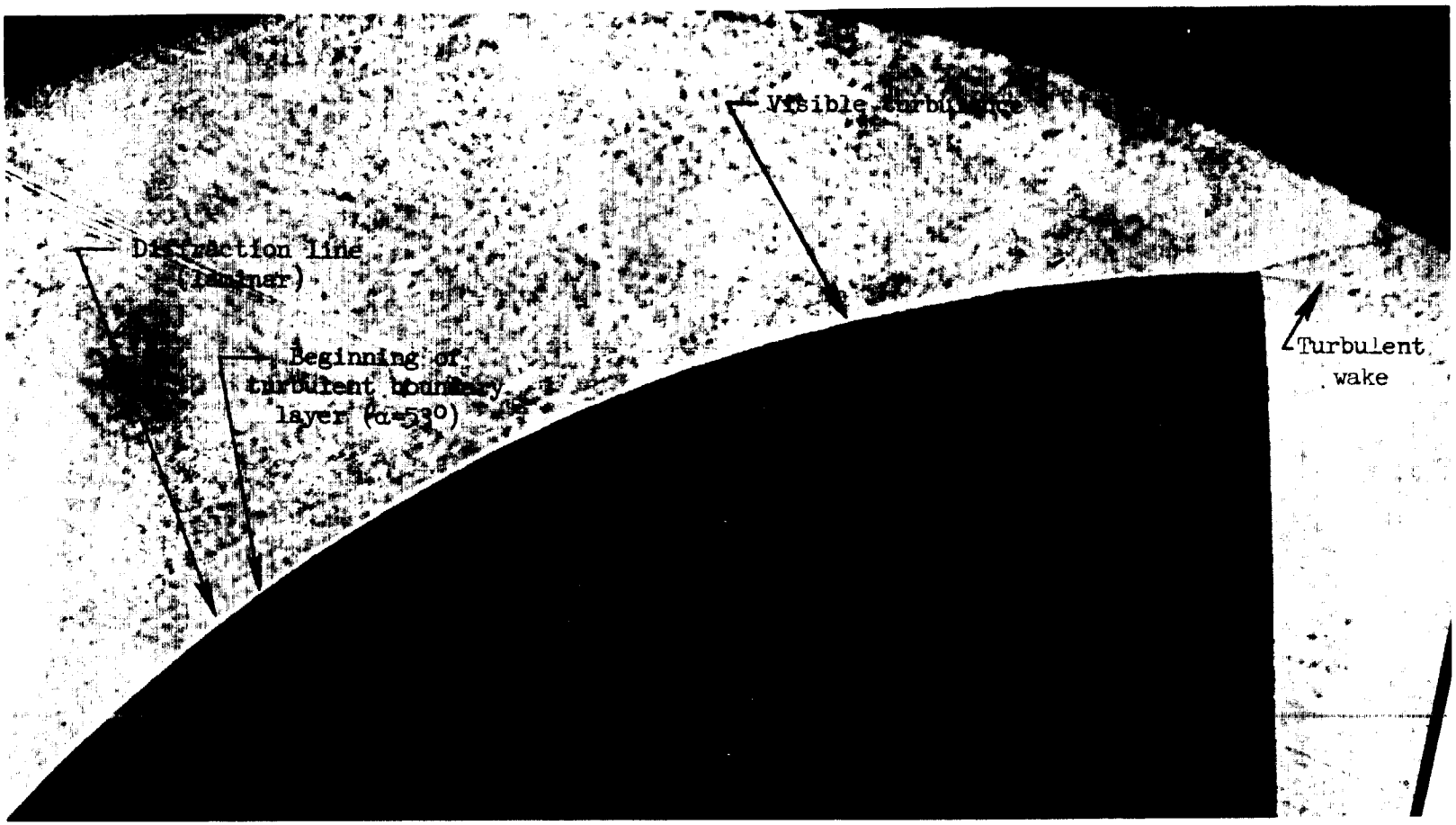

(c) Laminar and turbulent boundary layers; hemisphere A (after holes); k_{abs} = 2500; M_∞ = 2.48; R_{∞_D} = 6.4x10^6

Figure 3.- Concluded.

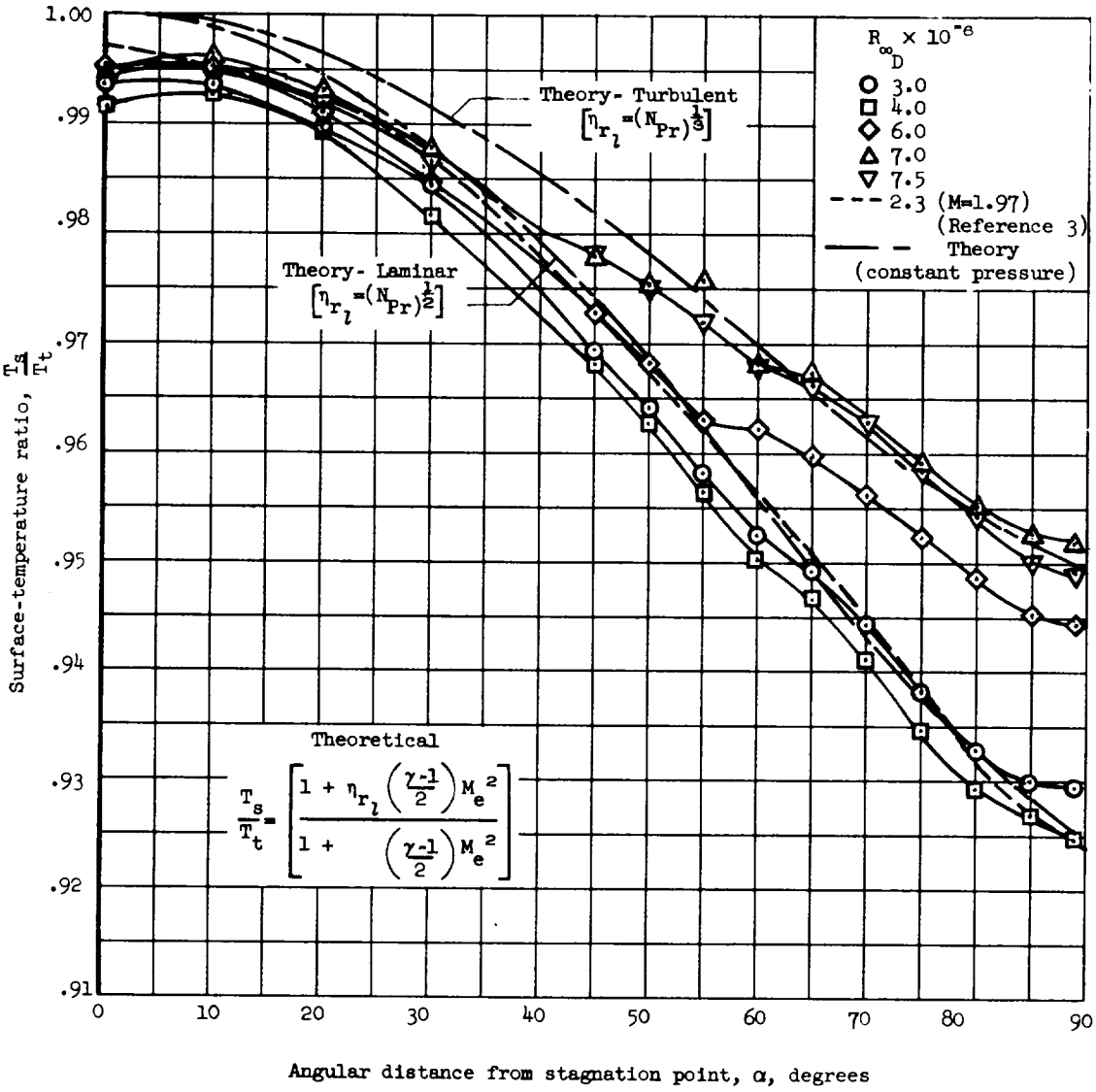

(a) Lower surface.

Figure 4.- Variation of surface-to-total-temperature ratio along surface of hemisphere at a Mach number of 2.48; absolute roughness = 580 microinches.

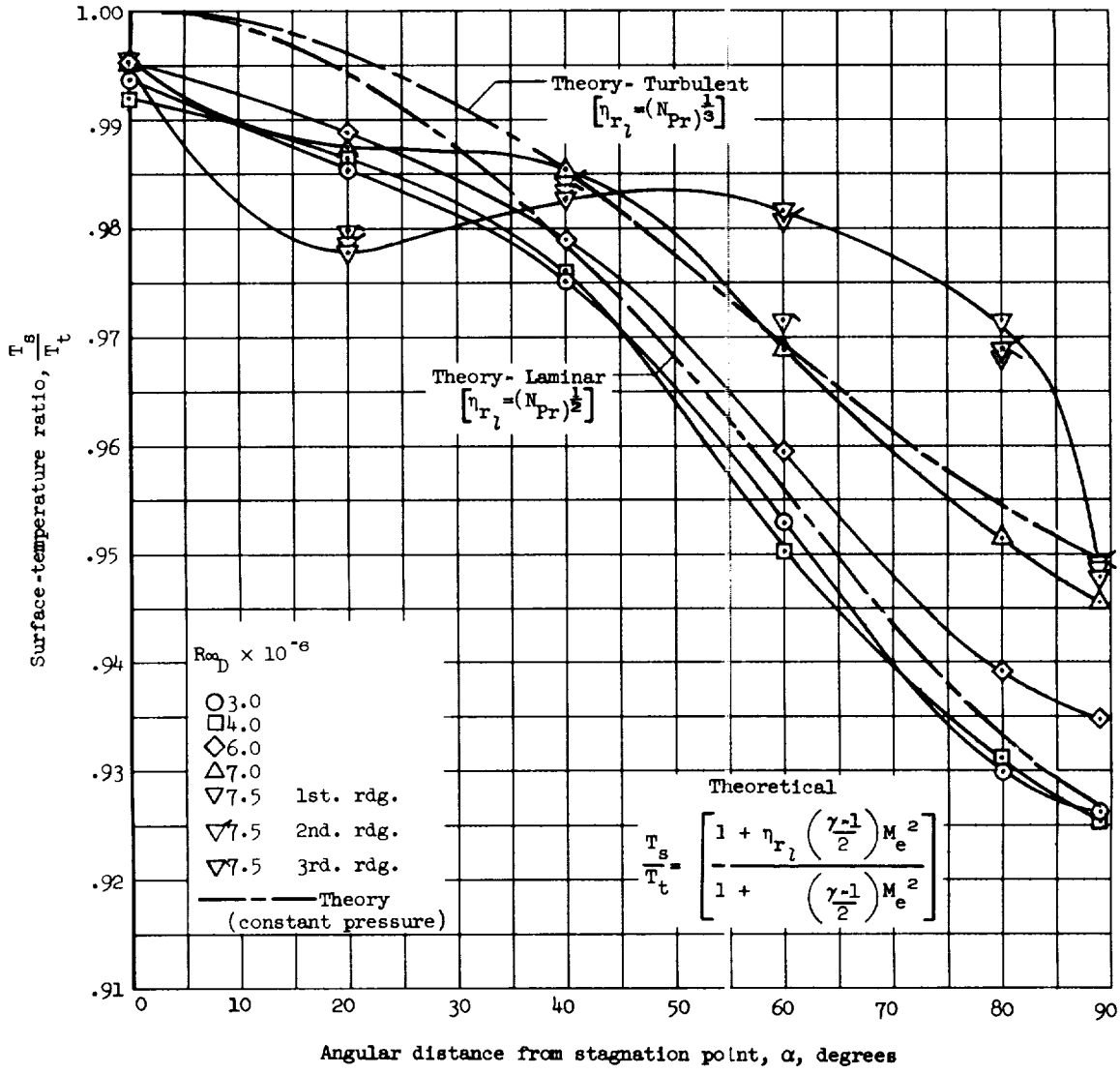

(b) Upper surface.

Figure 4.- Concluded.

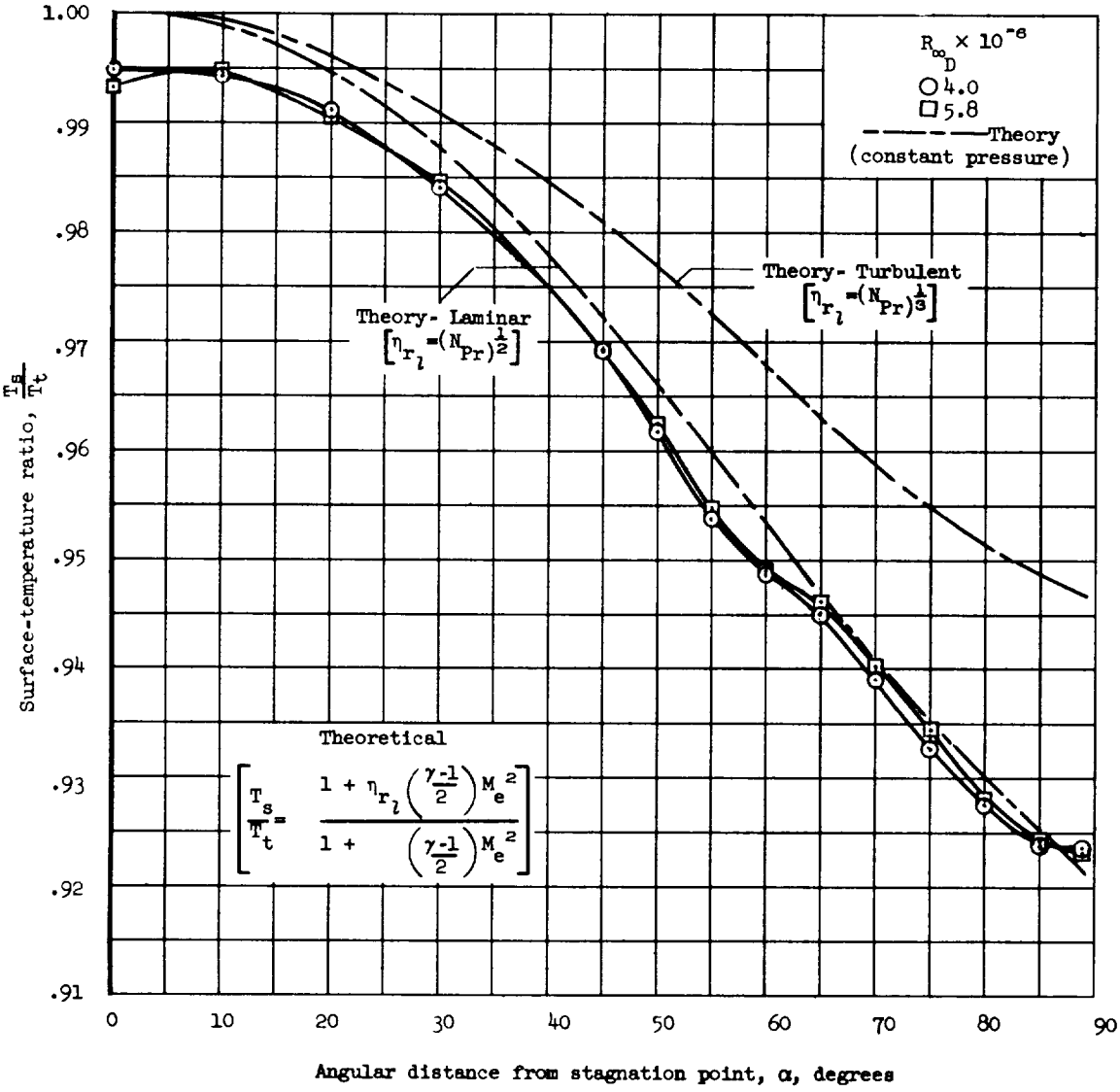

(a) Lower surface.

Figure 5.- Variation of surface-to-total-temperature ratio along surface of hemisphere at a Mach number of 3.07; absolute roughness = 580 microinches.

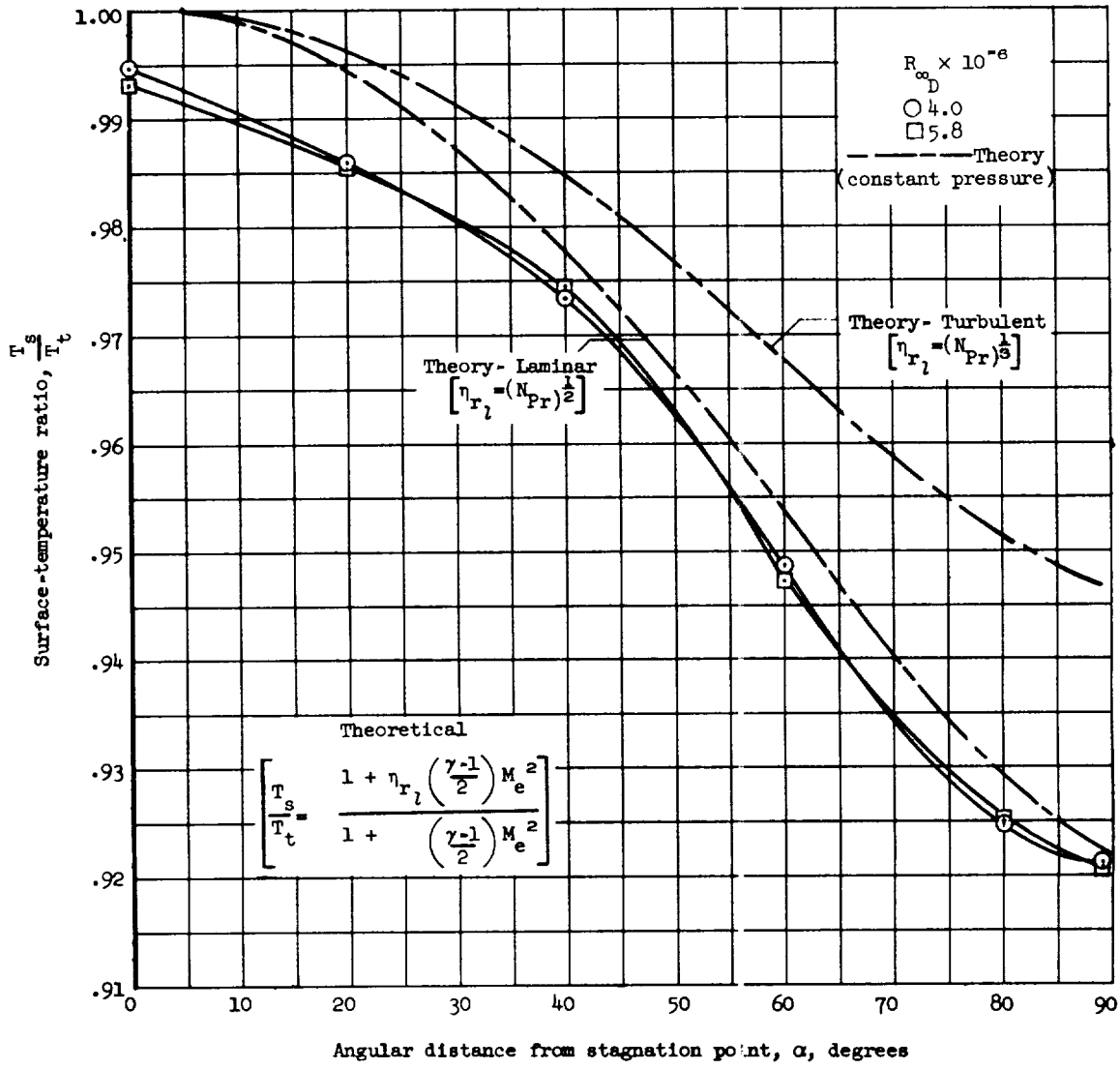

(b) Upper surface.

Figure 5.- Concluded.

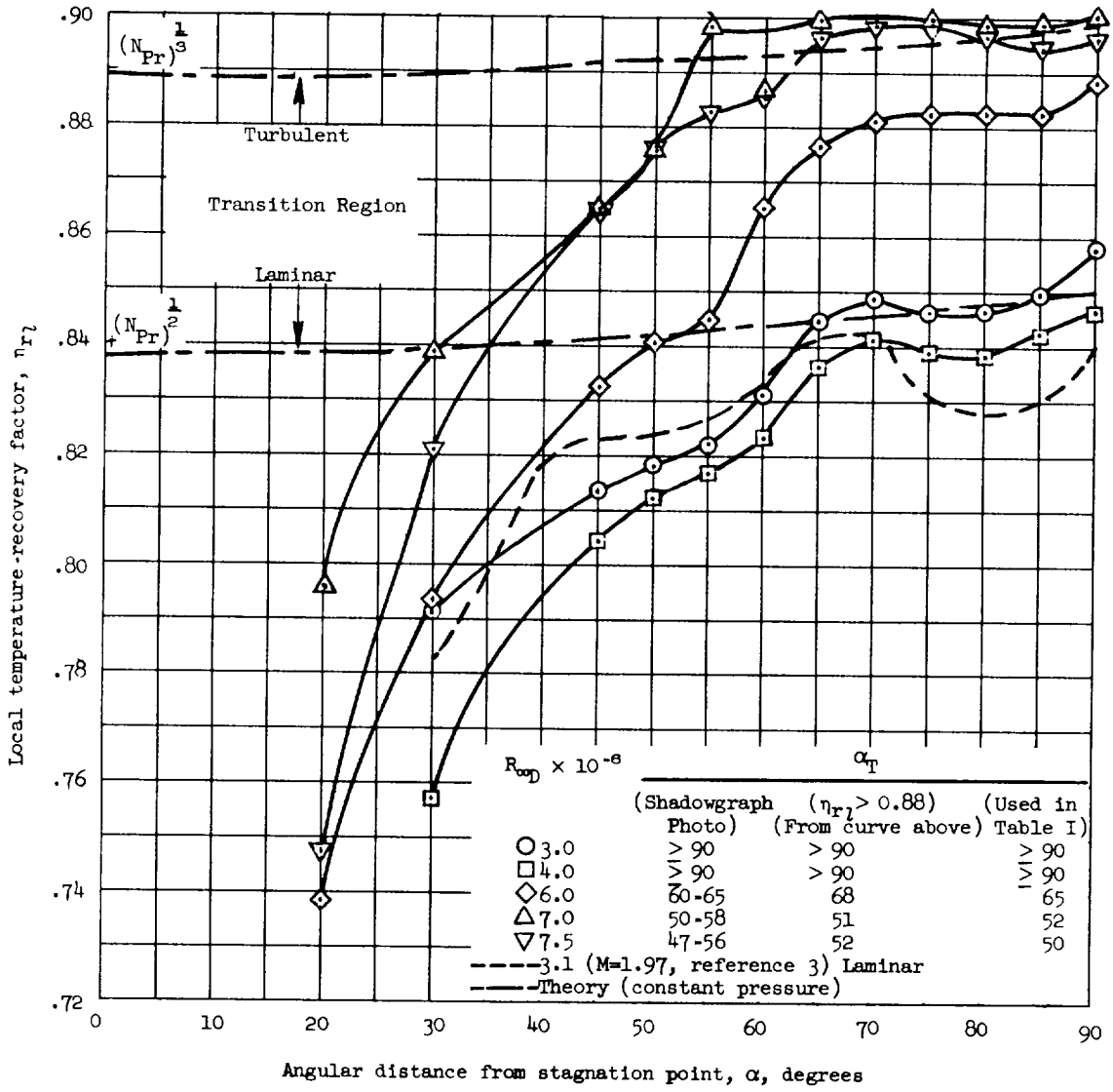

(a) Lower surface.

Figure 6.- Variation of local temperature-recovery factor along the surface of hemisphere at a Mach number of 2.48; absolute roughness = 580 microinches.

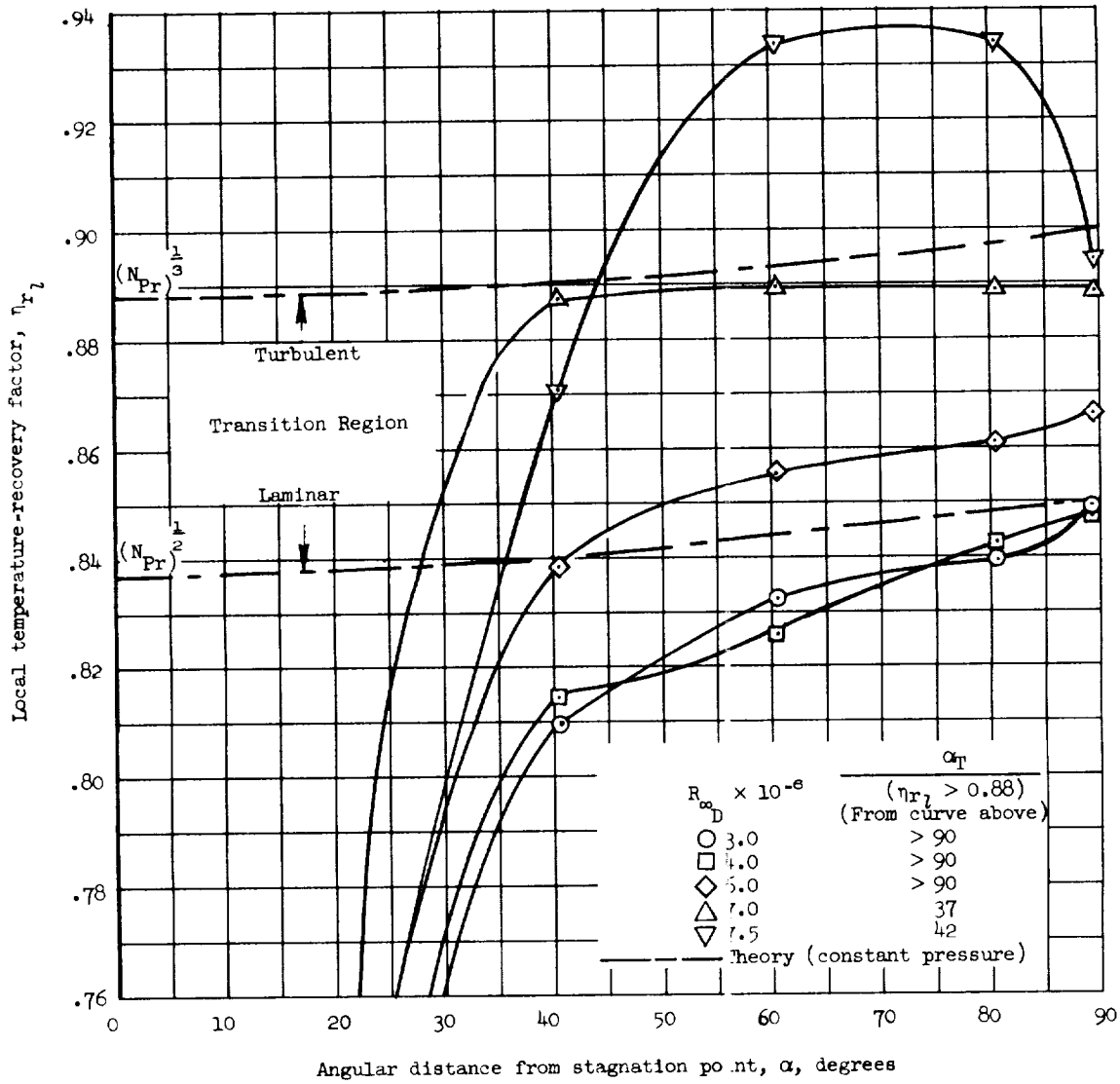

(b) Upper surface.

Figure 6.- Concluded.

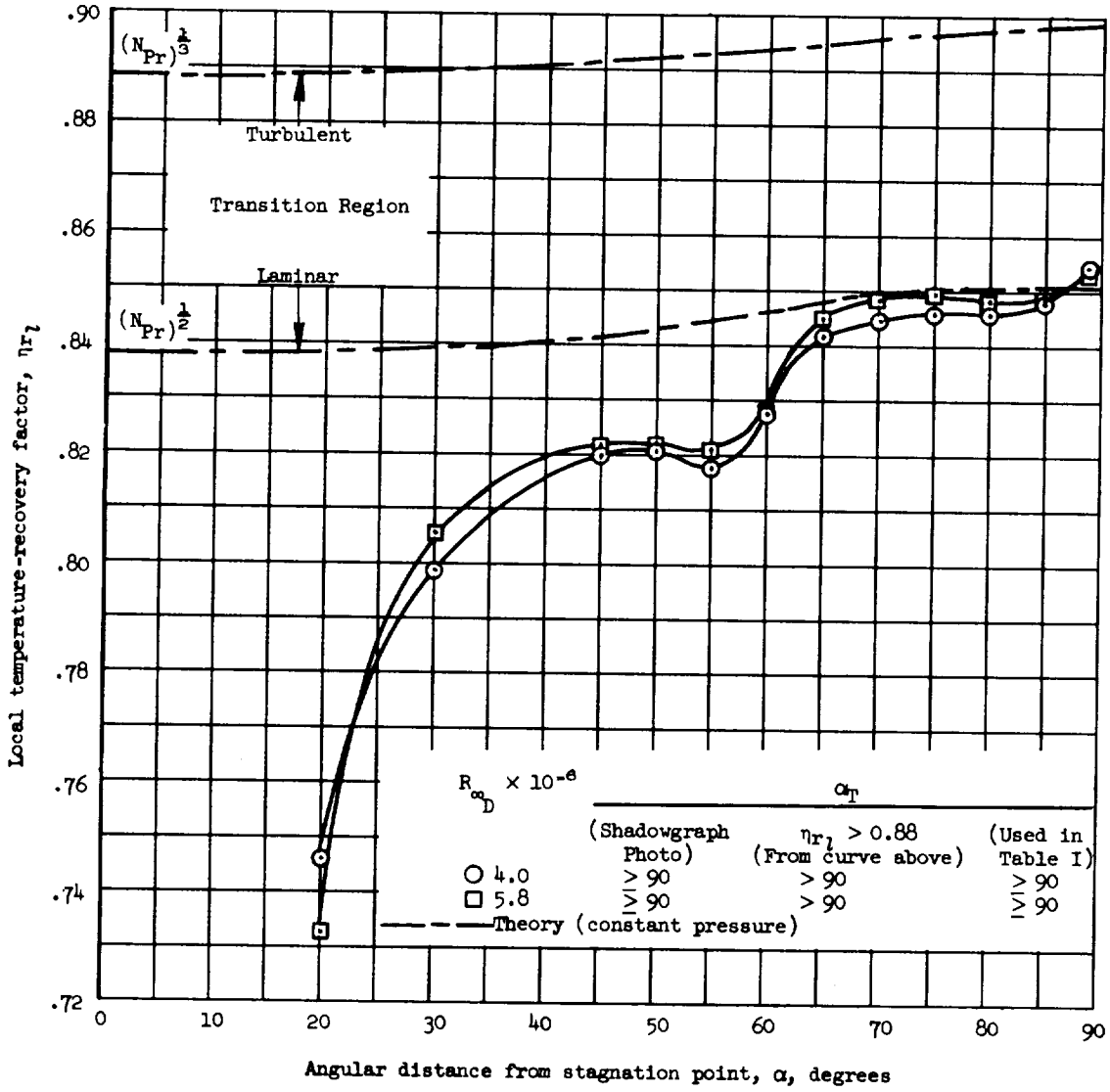

(a) Lower surface.

Figure 7.- Variation of local temperature-recovery factor along the surface of hemisphere at a Mach number of 3.07; absolute roughness = 580 microinches.

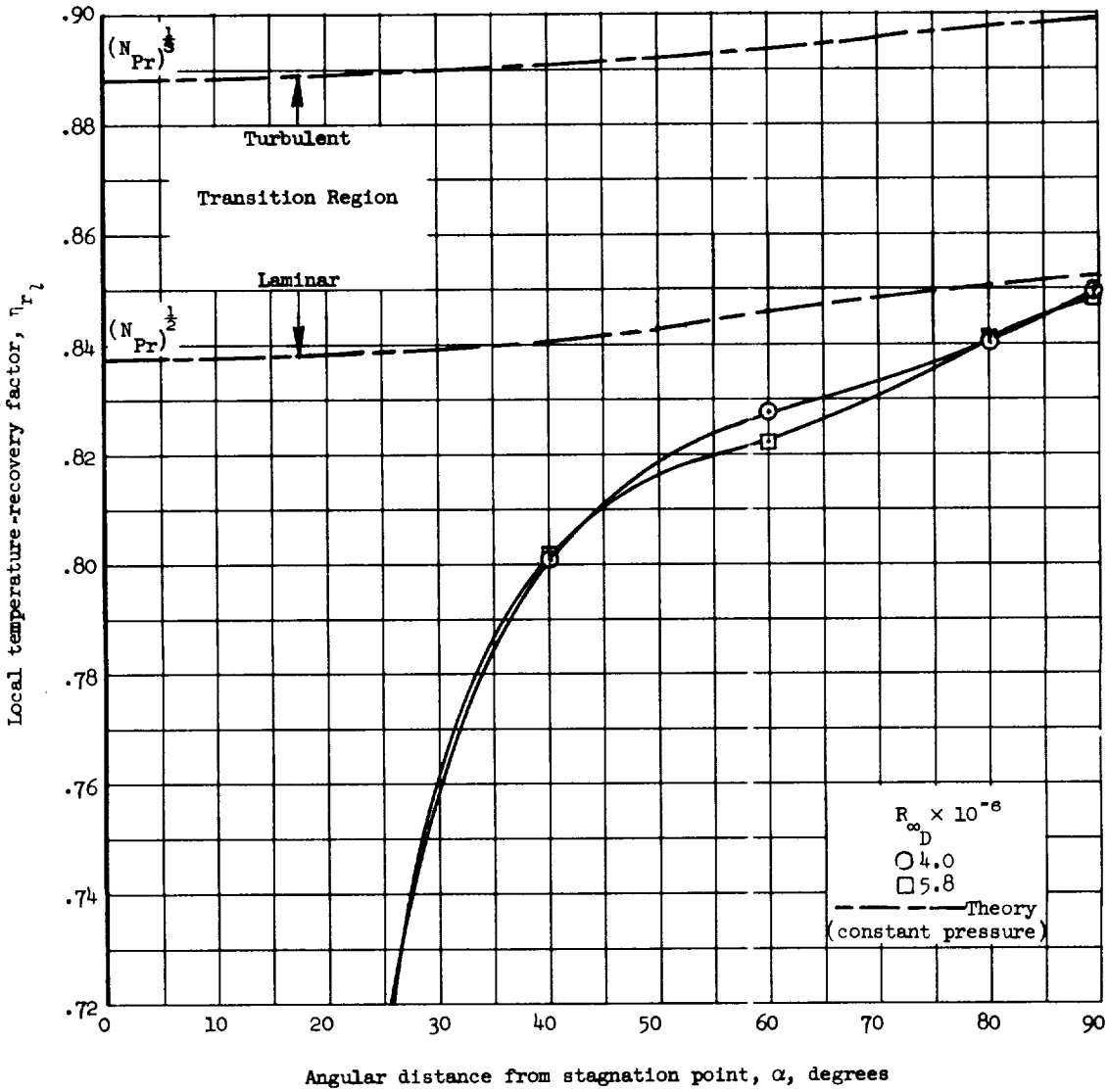

(b) Upper surface.

Figure 7.- Concluded.

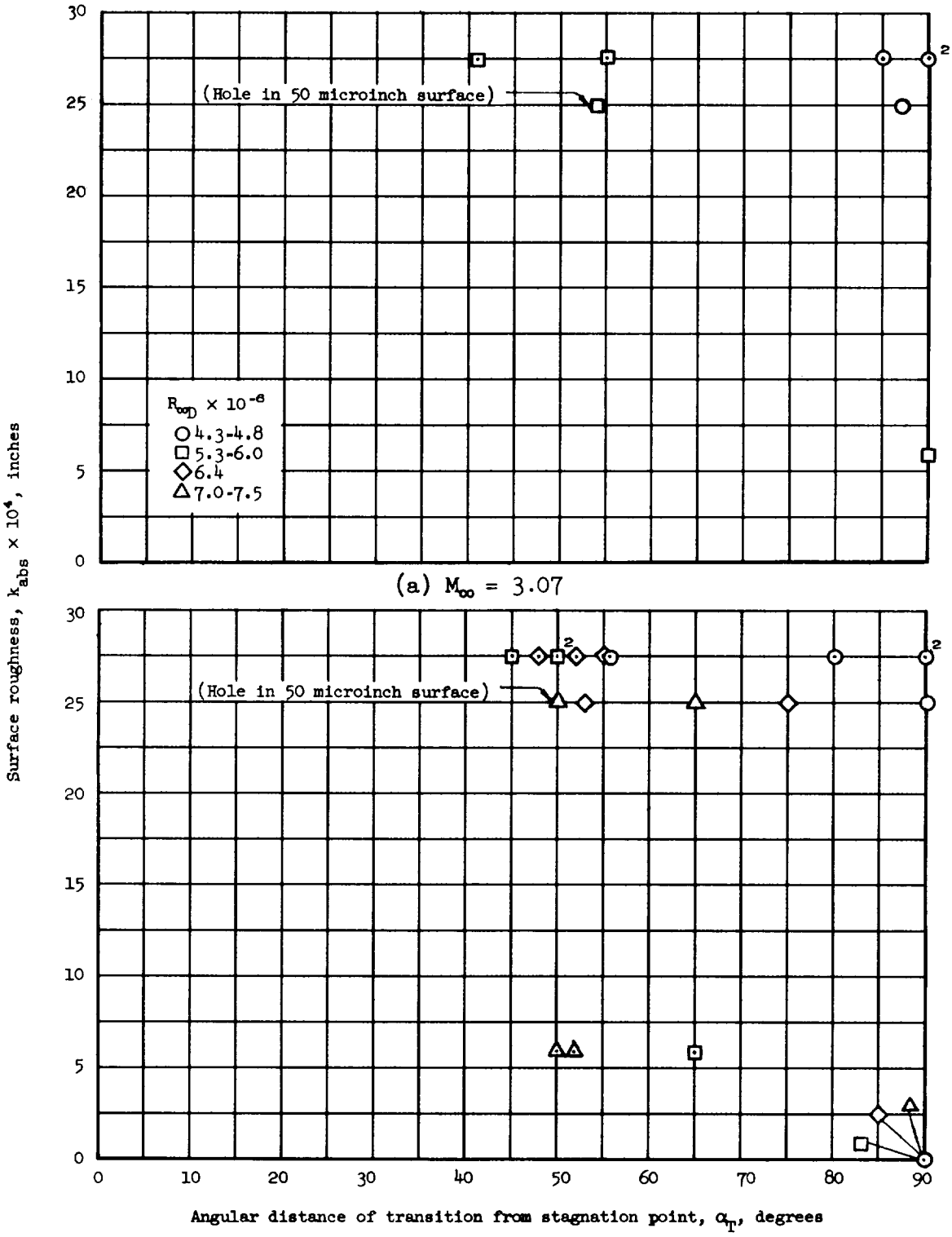

Figure 8.- Effect of surface roughness on location of transition.

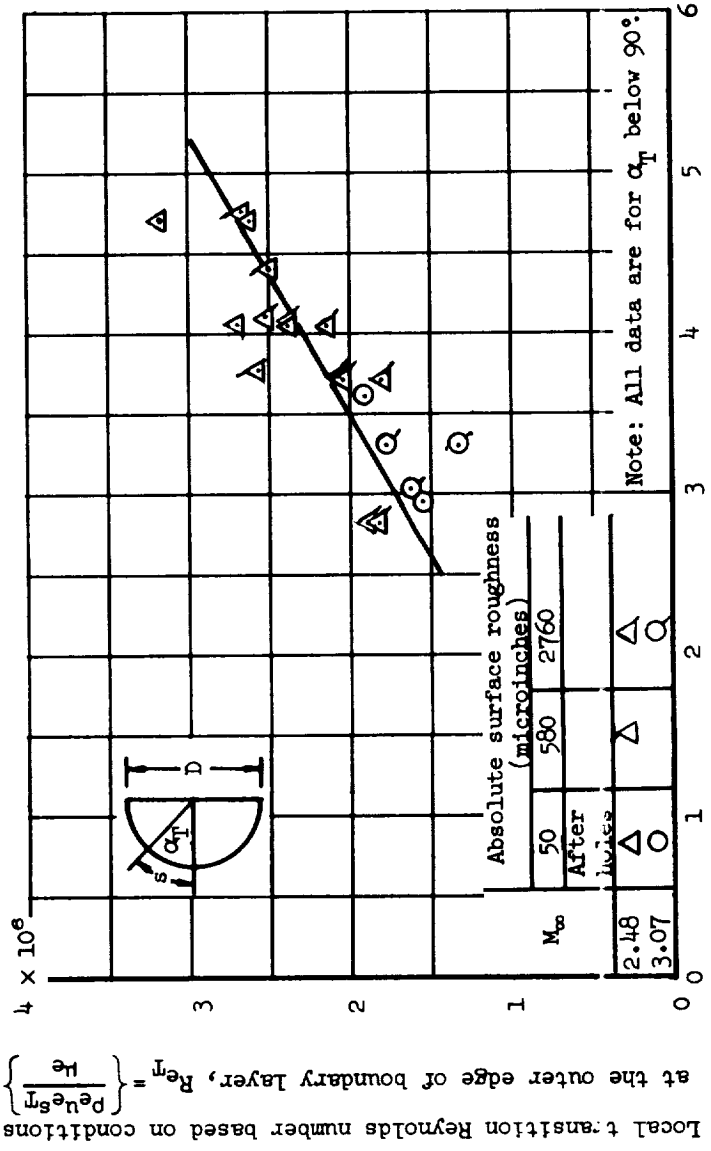

Figure 9.- Variation of local transition Reynolds number, based on conditions at the outer edge of the boundary layer, with stream Reynolds number per foot.

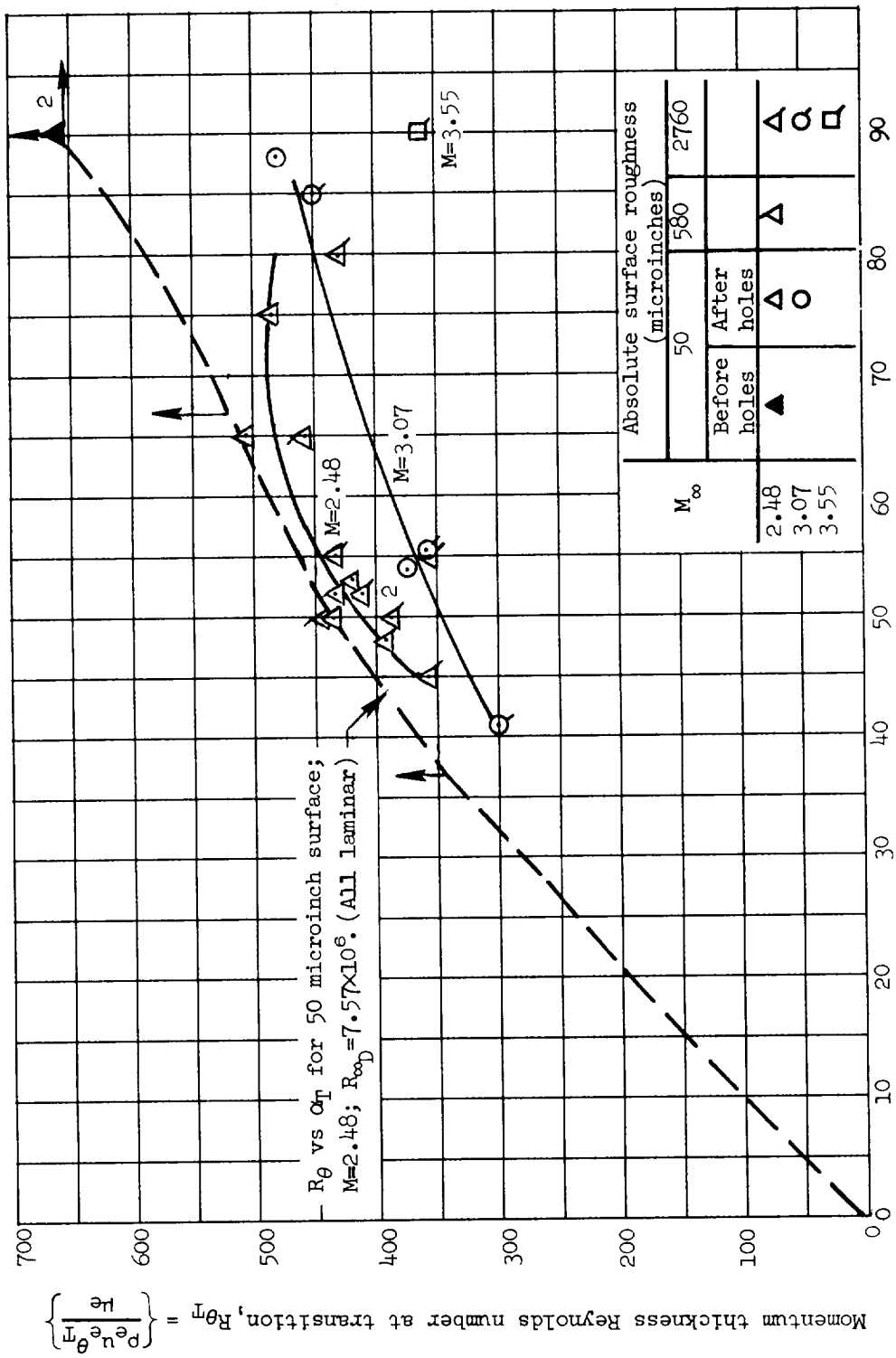

Figure 10.- Effect of surface roughness and Mach number on the variation of transition Reynolds number, based on momentum thickness, with angular location of transition.